ChemMedChem

Chemistry Europe
European Chemical Societies Publishing

Accepted Article

Title: Platinum(II) complexes bearing triphenylphosphine and chelating oximes: antiproliferative effect and biological profile in resistant cells

Authors: Mariafrancesca Hyeraci, Marialuigia Colalillo, Luca Labella, Fabio Marchetti, Simona Samaritani, Valeria Scalcon, Maria Pia Rigobello, and Lisa Dalla Via

To be cited as: *ChemMedChem* 10.1002/cmdc.202000165

Link to VoR: https://doi.org/10.1002/cmdc.202000165

WILEY-VCH

FULL PAPER WILEY-VCH

Platinum(II) complexes bearing triphenylphosphine and chelating oximes: antiproliferative effect and biological profile in resistant cells

Mariafrancesca Hyeraci,[a] Marialuigia Colalillo,[b] Luca Labella,[b] Fabio Marchetti,[b] Simona Samaritani,[b] Valeria Scalcon,[c] Maria Pia Rigobello[c] and Lisa Dalla Via*[a]

[a] Dr. M. Hyeraci, Prof. L. Dalla Via* 0000-0002-9828-9388
Department of Pharmaceutical and Pharmacological Sciences
University of Padova
Via F. Marzolo, 5, 35131 Padova (Italy)
E-mail: lisa.dallavia@unipd.it
[b] Dr. M. Colalillo, Prof. L. Labella, Prof. F. Marchetti, Prof. S. Samaritani
Dipartimento di Chimica e Chimica Industriale
Università di Pisa
Via G. Moruzzi 13, I-56124 Pisa, Italy
[c] Dr. Valeria Scalcon, Prof. Maria Pia Rigobello
Department of Biomedical Sciences
Università di Padova
Via U. Bassi 58/b, 35131 Padova, Italy

Supporting information for this article is given via a link at the end of the document.

Abstract: Platinum(II) complexes of the type $[Pt(Cl)(PPh_3)\{(\kappa^2\text{-}N,O)\text{-}(1\{C(R)=N(OH)\text{-}2(O)C_6H_4\})\}]$ with R = Me, H, (**1** and **2**) were synthesized and characterized. Single crystal X-ray diffraction confirmed for **1** the proposed (*SP*4-3) configuration. The study of the antiproliferative activity, performed on a panel of human tumor cell lines and on mesothelial cells, highlighted complex **2** as the most effective. In particular, it showed a remarkable cytotoxicity on ovarian carcinoma cells (A2780) and interestingly, a significant antiproliferative effect on cisplatin resistant cells (A2780cis). The investigation on the intracellular mechanism of action demonstrated for **2** a lower ability to platinate DNA with respect to cisplatin, taken as reference, and a notably higher uptake in resistant cells. A significant accumulation in mitochondria, along with the ability to induce concentration-dependent mitochondrial membrane depolarization and intracellular reactive oxygen species production, allowed us to propose a mitochondria-mediated pathway as responsible for the interesting cytotoxic profile of complex **2**.

Introduction

Cisplatin is a well-known metal-based chemotherapeutic agent, widely used for the treatment of a number of cancers such as: bladder, ovarian, testicular, non-small cell lung cancer, neuroblastoma and pleural mesothelioma.[1-3] Cisplatin enters into the cells through different mechanisms involving ion channels, active transporters or passive diffusion.[4,5] The main target responsible for its clinical effectiveness is the DNA,[6] which undergoes an irreversible damage due to covalent mono and diadducts formation which leads to the activation of repair pathways or cell apoptosis.[7]

Despite its wide utilization, cisplatin-based chemotherapies suffer of two main drawbacks: the occurrence of some dose-limiting side effects, mainly nephrotoxicity and neurotoxicity, and the occurrence of intrinsic or acquired resistance.[6] For this reason the search of new platinum complexes to improve clinical outcome of anticancer chemotherapies is still an attractive challenge among researchers. Resistance can occur through many different mechanisms, including reduced cisplatin uptake, increased detoxification by nucleophilic molecules, such as glutathione or metallothioneins, increased repair mechanisms or tolerance to platinum-DNA adducts, inactivation of apoptotic pathways.[8] In particular, failure of cell death plays an important role in resistant phenotype of cancer cells and being mitochondria key regulators of apoptosis, they could be considered an interesting target to overcome resistance phenomenon.[9-11]

Platinum complexes bearing both monodentate and chelating oxime ligands have been known for long[12,13] and recently some of them have showed interesting anticancer properties.[14-18] In an attempt to develop new promising platinum-based drugs, we have recently synthesized platinum(II) complexes bearing triphenylphosphine and bidentate aryloxime ligands $[Pt(Cl)(PPh_3)\{(\kappa^2\text{-}N,O)\text{-}(1\{C(R)=N(OH)\text{-}2(O)C_{10}H_6\})\}]$ (R = H, Me).[19] These complexes, characterized by a naphthalene residue on the oxime ligands, showed an interesting antiproliferative activity towards selected cancer cell lines: in particular, they were able to circumvent cisplatin resistance towards A2780cis cells. Moreover, it was shown that the hydroxyl group of oxime ligands can be alkylated under mild phase transfer catalysis experimental conditions,[19] opening the way to other functionalization pathways. Taking into account the interesting properties of this class of platinum(II) complexes, here we reported the synthesis, the characterization and the biological study of two structural analogues (complexes **1** and **2**), where the naphthyl group of oxime ligand was replaced by the smaller phenyl moiety. We have already observed, indeed, that biological properties can be modulated by the variation of certain residue dimensions.[20] The antiproliferative effect of **1** and **2** was assayed on a panel of human tumor cell lines, on the pairs A2780 and A2780cis, ovarian carcinoma cell lines, sensitive and resistant to cisplatin, respectively, and on mesothelial cells. The interaction of the most interesting complex **2** with DNA was analyzed, both quantitatively by ICP-AES technique, and

qualitatively, by electrophoretic mobility assay of supercoiled DNA, in comparison with cisplatin. The uptake and the intracellular distribution in resistant A2780cis cells were also determined. Finally, the effect on mitochondrial transmembrane potential, and the ability to produce intracellular reactive oxygen species were evaluated.

Results and Discussion

Chemistry

The preparation of complexes **1** and **2** was carried out starting from dinuclear *trans*-[Pt(μ-Cl)Cl(PPh_3)]$_2$[21] and the suitable bidentate oxime ligand (Pt/oxime = 1.0 molar ratio), in the presence of silver acetate (Scheme 1). Although the reaction proceeds toward the chelated complex even in the absence of a dehalogenation agent,[19] the addition of silver acetate makes the process much faster. The initial bridge splitting of the dinuclear precursor by the oxime is guided by *trans* effect of PPh_3 ligand. Although when monodentate oxime ligands are used isomerization of the kinetic trans product is often observed in solution[22] in this case the bridge splitting is followed by the fast chelation step, thus a single product is observed. The complexes were recovered in good yields and their characterization (elemental analysis, IR, ^{1}H, ^{31}P, ^{13}C and ^{195}Pt NMR) was in good agreement with the proposed structure. As an example, the main spectroscopic features of complex **1** can be briefly discussed. In the ^{31}P NMR spectrum, a single signal with satellites is present at 6.65 ppm ($^1J_{P\text{-}Pt}$ = 3959Hz), while in the ^{195}Pt NMR spectrum a doublet with the same coupling constant was observed at -2984 ppm, in good agreement with analogous complexes.[19] The presence of a single isomer was evident also in the ^{1}H NMR spectrum, where a single singlet for CH_3 methyl group of ketoxime ligand was observed at 2.51 ppm. In the case of **1** single crystal X-ray diffraction confirmed the (*SP*4-3) configuration. The complexes are well soluble in DMSO/H_2O 95/5 v/v and could be stored at -18 °C in these conditions.

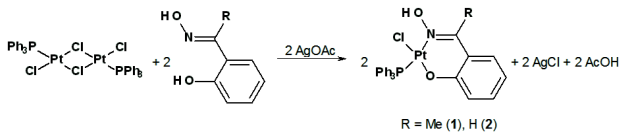

Scheme 1. Synthesis of the new **1** and **2** complexes.

The molecular structure of **1** is reported in Figure 1, while the most significant bond lengths and angles are listed in Table 1. The coordination around platinum is square planar, with small deviations from ideality. The oxime ligand chelates the metal by the oxime nitrogen atom and the anionic phenol oxygen in position 2' of the phenyl ring, while the remaining two positions around the metal center are occupied by a chloride ion and a triphenylphosphine ligand. Pt-O and Pt-N bond lengths are in good agreement with those previously reported for (*SP*4-3)-[Pt(Cl)(PPh_3){(κ^2-*N,O*)-[(1E)-2-hydroxynaphthalene-1-carbaldehyde oxime]}][19] and can be compared with bond lengths reported by Kaplan et al.[23] for the complex [Pt(*o*-$OC_6H_4CH{=}NOH)_2$]. While Pt-O bond length is analogous (1.984(3) *vs* 1.978(5) Å), Pt-N bond is slightly longer in **1** (2.063(4) *vs* 1.974(6) Å), due to the presence of a triphenylphosphino ligand in *trans* position. A non bonding interaction between the oxime hydroxyl group and the coordinated chloride is present, as shown by the measured O(2)...Cl(1) short distance (2.953(3) Å).

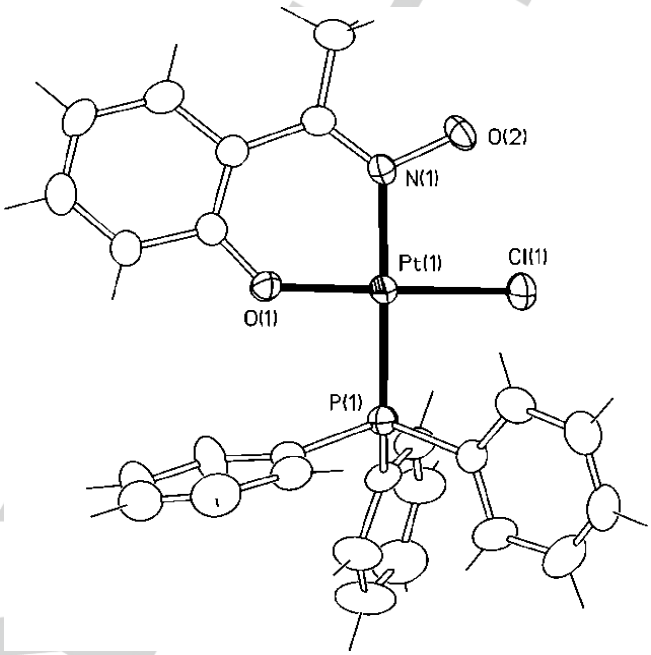

Figure 1. Molecular structure of **1**.

Table 1. Bond lengths [Å] and angles [°] for complex **1** (PLACHOX).

Pt(1)-O(1)	1.984(3)	O(1)-Pt(1)-N(1)	89.13(13)
Pt(1)-N(1)	2.063(4)	O(1)-Pt(1)-P(1)	88.68(9)
Pt(1)-P(1)	2.2536(12)	N(1)-Pt(1)-P(1)	176.77(10)
Pt(1)-Cl(1)	2.3153(13)	O(1)-Pt(1)-Cl(1)	179.26(11)
N(1)-C(7)	1.290(5)	N(1)-Pt(1)-Cl(1)	90.49(10)
N(1)-O(2)	1.396(4)	P(1)-Pt(1)-Cl(1)	91.67(5)
		C(7)-N(1)-O(2)	113.5(3)
		C(7)-N(1)-Pt(1)	129.7(3)
		O(2)-N(1)-Pt(1)	116.6(3)

Antiproliferative activity

The effect of the new complexes on cell growth was investigated on a panel of human tumor cell lines, on cisplatin sensitive (A2780), and resistant (A2780cis) ovarian carcinoma cells and on non tumorigenic mesothelial cells (MeT-5A). The cisplatin was taken into consideration as reference. The obtained results, expressed as IC_{50} values, i.e. the concentration of complex able to provoke 50% cell death with respect to a control culture, are listed in Table 2. The cytotoxicity profiles for **1** and **2** are shown in Figure S9.

The obtained IC_{50} values indicate for both complexes an interesting antiproliferative effect characterized by low micromolar values in most cancer cell lines and in the non tumorigenic MeT-5A and for **2** a higher cytotoxic activity with respect to **1**. Interestingly, on lung carcinoma (A549) and colorectal adenocarcinoma (HT-29) cells, **2** shows an effect comparable to that induced by the reference drug, while on ovarian carcinoma cells, i.e. A2780, the cytotoxicity induced by the new complex is even higher with respect to that of cisplatin. Moreover, in these latter cells the antiproliferative activity of the new complexes is also higher with respect to that induced on MeT-5A.

Table 2. Cell growth inhibition in the presence of **1**, **2** and cisplatin, taken as reference.

Complex	Cell Line IC_{50}[a] (μM)							RF[b]
	HeLa	A549	HT-29	MSTO-211H	A2780	A2780cis	MeT-5A	
1	3.87± 0.38	5.18± 0.48	3.83± 0.36	14.1± 1.6	0.62± 0.16	1.43± 0.36	3.15± 0.61	2.3
2	2.47± 0.40	2.50± 0.70	2.63± 0.82	3.61± 1.16	0.31± 0.03	1.08± 0.41	2.60± 0.52	3.5
cisplatin	1.51± 0.09	2.10± 0.25	2.57± 0.67	1.35± 0.22	0.91± 0.13	6.61± 0.61	nd[c]	7.3

[a] Cells were incubated in the presence of tested complexes for 72 h and the IC_{50} values are the mean ± SD of at least three independent experiments. [b] $RF=IC_{50}(A2780cis)/IC_{50}(A2780)$. [c] not determined

As regards the resistant variant cells A2780cis, both **1** and **2** exert a noteworthy antiproliferative activity. Indeed, in this cell line the most active **2** shows an IC_{50} value in the low micromolar range and about six times lower than that obtained for the drug. Moreover, the comparison between the cytotoxicity obtained for the sensitive (A2780) and the resistant (A2780cis) cells highlighted for cisplatin, as expected, a decrease of about seven times of the cell effect (RF=7.3), whilst for **2** a lower decrement, about three times (RF=3.5), was observed. These results suggest that **2**, along with the ability to exert a remarkable cytotoxicity, is also able to overcome, at least partially, the resistance phenomenon in ovarian carcinoma cells.

Interaction with DNA

On the basis of the interesting antiproliferative effect shown by these complexes on tumor cells, and in particular, on resistant A2780cis, we decided to investigate their possible intracellular target(s). In particular, the complex **2** was taken into consideration due to the low IC_{50} values. It is well known that the main intracellular target of cisplatin is DNA and that the most successful platinum-containing drugs introduce covalent adducts in the macromolecule.[7] In this connection, the ability of **2**, and for comparison of cisplatin, to platinate the macromolecule was determined by ICP-AES technique. For this purpose, salmon testes DNA was incubated up to 48 hours in the presence of test complexes at [DNA]/[complex] ratio equal to 10, and the results, expressed as ppb, are shown in Figure 2.

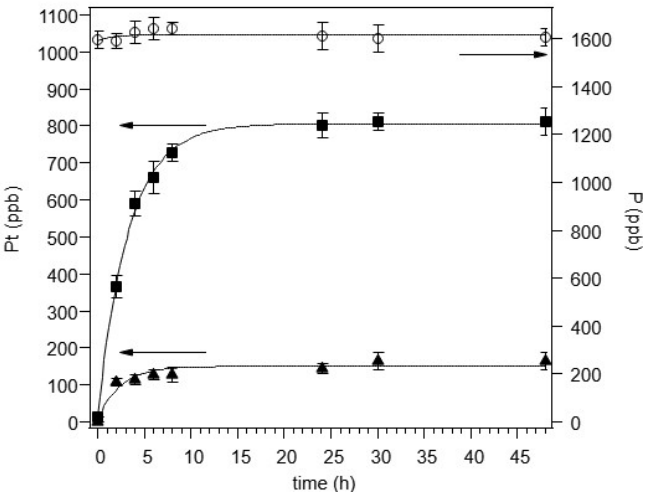

Figure 2. Platinum (full symbols) and phosphorus (empty circles) bound to salmon testes DNA incubated in the presence of **2** (triangles) or cisplatin (squares) as a function of incubation time (0-48 h). [DNA]=9 x 10^{-4} M, [DNA]/[complex]=10. Mean values ± SD of five experiments are reported.

Both **2** and the reference drug show a saturation behavior that becomes practically complete within 10 hours of incubation, otherwise, the total amount of Pt bound to DNA appears significantly different. In detail, in the presence of cisplatin, about 800 ppb are detected after 48 hours, while for **2** the maximum amount of platinum bound to the macromolecule is about 150 ppb. This considerable difference could result from a potential behavior of complex **2** as monodentate ligand for DNA and from the presence of the bulky PPh_3 group.

To further assess the results shown in Figure 2, the interaction of **2** and the drug with the macromolecule was analyzed also by electrophoretic mobility assay of plasmid DNA. In detail,

supercoiled pBR322 DNA was incubated for 24 hours at 37 °C in the presence of test complexes and the degree of supercoiling was monitored by agarose gel electrophoresis (Figure 3).

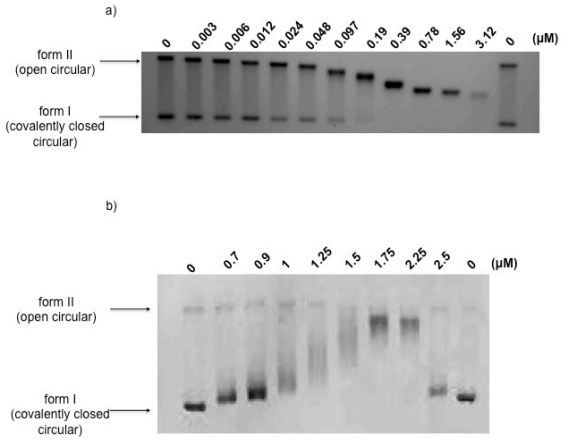

Figure 3. Gel electrophoresis mobility of pBR322 plasmid DNA incubated for 24 hours at 37 °C in the presence of cisplatin (a) or **2** (b) at the indicated concentrations (μM). A representative experiment (from three independent replicates) is shown.

In the presence of increasing concentrations of cisplatin, the migration rate of supercoiled form I gradually decreases, while the mobility of the open circular form II accelerates, until a coalescence point is observed at 0.78 μM concentration (Figure 3a). It is to note that the occurrence of a coalescence point is retained the consequence of a strong unwinding of supercoiled DNA and, actually, it can be detected when complete removal of supercoils from plasmid DNA occurs.[24] The incubation of pBR322 plasmid with **2** gives rise to a quite different behavior (Figure 3b). Indeed, only a slight increase in the mobility of form II is detected and higher concentrations of the complex are needed to obtain the co-migration of both forms with respect to cisplatin, thus confirming a less effective interaction with the macromolecule.

As a consequence, DNA could not be the main responsible for the antiproliferative activity exerted by **2**, and then, to identify other possible target(s), the mechanism of action of **2** was further investigated.

Cell uptake

Notwithstanding the cisplatin resistance must be considered a multifactorial event, one of the most prominent features of such phenomenon is constituted by a reduced intracellular drug accumulation.[25,26] In this connection, we evaluated in A2780cis cells the uptake of **2** and cisplatin, as a function of incubation time (0 to 180 minutes). For this purpose, cells were incubated in the presence of 100 μM test agent, and the amount (in ppb) of platinum and phosphorus was measured by ICP-AES (Figures 4a and b).

The obtained data demonstrated for A2780cis cells a remarkably higher ability to accumulate **2** with respect to cisplatin (Figure 4a vs 4b), and, interestingly, this result appears in agreement with the higher antiproliferative effect exerted by the oxime complex (see Table 2). In detail, after 3 hours of incubation, the amount of platinum in A2780cis cells incubated with **2** is about 30-folds that determined in cells treated with the reference drug. As regards the phosphorus content, it slightly decreases during the incubation with **2**, leading to a reduction of about 14% with respect to the total, and this could be attributed to the significant cytotoxic effect of the test complex (Figure 4a). Otherwise, the cisplatin does not induce any appreciable difference in phosphorus content within the different samples during the overall time of the experiment, so confirming its lower effect on cell viability (Figure 4b). Such difference in uptake between the two complexes is likely due to the higher lipophilicity of **2** with respect to the drug and could further support the assumption that intracellular target(s) other than DNA could be involved in the antiproliferative effect of **2**.

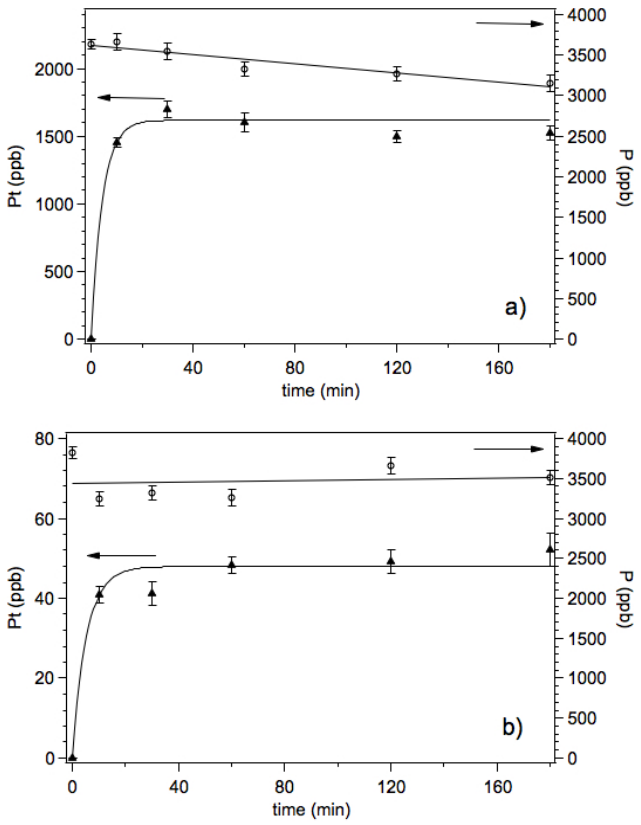

Figure 4. Platinum (full symbols) and phosphorus (empty circles) in A2780cis cells incubated in the presence of 100μM **2** (a) or cisplatin (b) as a function of incubation time (0-180 min). Mean values ± SD of four experiments are reported.

Mitochondria transmembrane potential (ΔΨ) and intracellular compartmentalization

Among the phenotypic changes that contribute to the development of anticancer drug resistance, the inactivation of the apoptosis pathway plays a relevant role[10,8,27,28] and inside the cell, mitochondrion represents the key organelle in the control of the apoptotic machinery. As a consequence, mitochondria have been proposed as interesting potential targets in anticancer therapy and the development of mitochondria-targeted agents emerged as a promising approach to face drug resistance.[9-11] Accordingly, a considerable interest has been directed toward the so-called “mitochondriotropic”

agents.[29] Actually, a number of clinically approved drugs as well as experimental anticancer agents, demonstrated the capacity to interfere with mitochondrial functions, promoting the apoptotic phenomenon.[9,10,30,31] Moreover, in previous papers we demonstrated the ability of some Pt(II) complexes to affect mitochondria, leading to apoptosis.[32,20] In this connection, it appeared of interest to investigate the effect of **2** on mitochondrial transmembrane potential ($\Delta\Psi$) in A2780cis cells treated with different concentrations of the test agent and stained with the fluorescent cationic probe JC-1. The obtained results, shown in Figure 5, clearly indicate the capacity of **2** to promote a concentration-dependent depolarization of the mitochondrial membrane.

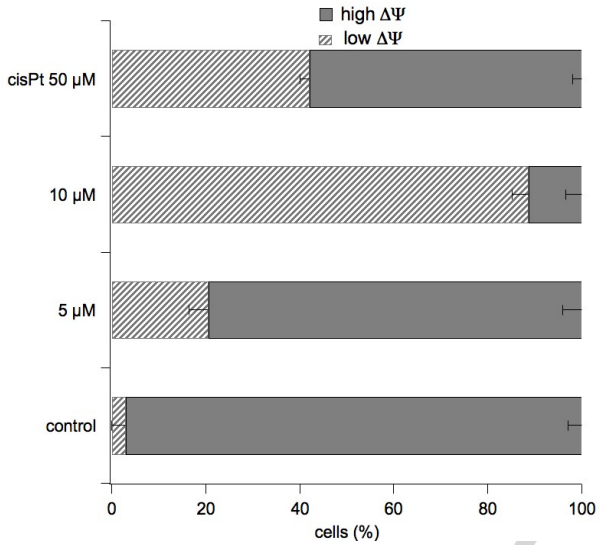

Figure 5. Cytofluorimetric analysis of mitochondrial transmembrane potential ($\Delta\Psi$). A2780cis cells were incubated for 28h in the presence of **2** or cisplatin (cisPt) at the indicated concentrations and stained with JC-1. Mean values ± SD of three experiments are reported

In detail, in the control condition, about 96% of A2780cis cells show a high $\Delta\Psi$. In the presence of 5 μM **2** about 22% of cells exhibit a significant decrease in $\Delta\Psi$ and a more marked effect is observed at 10 μM concentration: indeed, in this latter experimental condition almost 90% of cells undergo mitochondrial depolarization. Interestingly, the effect of cisplatin appears notably weaker with respect to that provoked by **2**, because a drug concentration of 50 μM is needed to induce mitochondrial membrane depolarization in about 40% of A2780cis cells.

The above results suggest mitochondria as a possible intracellular target responsible of the cytotoxic effect of **2**. To further support this hypothesis, we investigated the sub-cellular distribution of the complex. For this purpose, whole A2780cis cells were incubated for 3 hours in the presence of 100 μM test complex or cisplatin, and the content in ppb of platinum and phosphorus in mitochondria- and cytosol-enriched fractions was determined by ICP-AES analysis. The obtained data were expressed as platinum /phosphorus ratio ([Pt]/[P]) for both cell fractions (Figure 6a). It is to underline that phosphorus content can be considered as internal standard and actually, a linear correlation between cell number and ppb of phosphorus has been previously verified (data not shown).

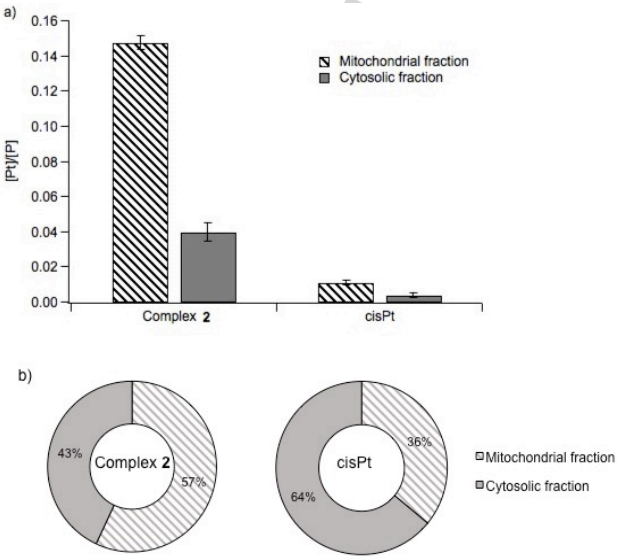

Figure 6. Platinum/Phosphorus (ppb) ratio ([Pt]/[P]) (a) and platinum (ppb) accumulation (b) in mitochondria- and cytosol-enriched fractions obtained from A2780cis cells incubated for 3 h in the presence of 100 μM **2** or cisplatin. Mean values ± SD of three experiments are reported.

The comparison between the [Pt]/[P] values obtained by incubating cells with **2** or cisplatin highlights interesting differences (Figure 6a). In details, the fractions obtained from cells incubated with **2** show [Pt]/[P] values clearly higher with respect to those in the presence of drug, indicating that **2** is accumulated more easily into A2780cis cells with respect to cisplatin. Interestingly, this result is in accordance with the data of cell uptake shown in Figure 4. Moreover, for **2** the [Pt]/[P] value in mitochondria-enriched fraction is about 3.8-fold higher than that in the cytoplasm one, while for cisplatin, such difference is about 2.6-fold. The percentages of platinum accumulation (ppb) in mitochondria- and cytosol-enriched fractions are also reported (Figure 6b), confirming for **2** a higher accumulation in mitochondria with respect to the drug. Therefore, for **2** a more efficient compartmentalization in mitochondria can be assumed. It is well-known that lipophilic cations preferentially accumulate in mitochondria and the attachment of the lipophilic triphenylphosphine ligand was considered a strategy to target bioactive molecules to mitochondria.[33-36] Indeed, the polarization of PPh_3 ligand upon metal coordination could be considered similar to that of PPh_3 residue in triphenylphosphonium cations, since in both cases the phosphine lone pair is involved in a sigma-donating bond. Moreover, it is likely that inside the cell the hydrolysis of platinum-chlorine bond takes place, generating a cationic aquo complex. The results in Figure 6 appear in agreement with these considerations and the triphenylphosphine moiety could be retained the main responsible for the high uptake in cell and the affinity toward mitochondria observed for **2**.

ROS production

Mitochondria are the main intracellular source of endogenous Reactive Oxygen Species (ROS, i.e. superoxide anion and hydrogen peroxide).[37] The maintenance of a correct redox balance is crucial for the cell. Indeed, ROS are essential for the regulation of many physiological processes and cell signaling, and also play a central role in apoptosis.[36,38,39] The ability of **2** to localize in mitochondria (Figure 6) and to induce mitochondrial membrane depolarization (Figure 5) prompted us to verify if the test agent could be able to affect the production of mitochondrial ROS, triggering intracellular oxidative stress. In this connection, we measured short-term (0-120 min) ROS production in A2870cis cells loaded with chloromethyl 2',7'-dichlorofluorescein diacetate and incubated in the presence of increasing concentrations of **2** (10-100 μM). The obtained results, expressed as percentage of fluorescence intensity after 120 min of incubation, with respect to the control, are shown in Figure 7. 100 μM Cisplatin was used as reference.

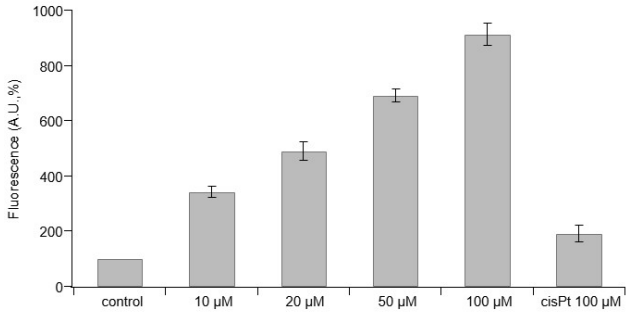

Figure 7. ROS production in A2780cis cells incubated with **2** or cisplatin (cisPt) at indicated concentrations for 120 minutes. The experiments were performed with eight biological replicates. Mean values ± SD are reported.

In the presence of **2**, the A2780cis cells show a notable dose-dependent increase in ROS production, significantly more pronounced with respect to that induced by cisplatin. Taking into consideration that high doses of ROS have been linked to the activation of some intracellular components of the apoptotic pathway,[39] it could be hypothesized that the production of ROS induced by **2** play a crucial role in the cytotoxic effect of this complex.

Conclusion

The synthesis and characterization of two platinum(II) complexes (**1** and **2**) bearing triphenylphosphine and bidentate aryloxime ligands are described, and for complex **1** the molecular structure was assigned by single crystal X-ray diffraction. In particular, complex **2** showed an interesting biological profile by exerting an antiproliferative effect on human tumor cell lines higher than that of the reference drug, cisplatin, and notably, by inducing a noteworthy cytotoxicity on cisplatin-resistant ovarian cancer cells. The ability to be efficiently accumulated in resistant cells is accompanied by a scarce covalent interaction with DNA and interestingly, by a significant localization in mitochondria. The ability to provoke a concentration-dependent depolarization of transmembrane mitochondrial potential and a remarkable reactive oxygen species production inside the cells, allowed us to assume mitochondria as the potential intracellular target of this complex. The development of new antitumor drugs capable to overcome the resistance phenomenon and endowed with lower capacity to interact with DNA still represents a challenge and a desirable goal inside the antitumor chemotherapy. Indeed, such agents could demonstrate a reduction of the mutagenic effect, caused by many conventional anticancer drugs, and responsible of secondary malignancies as well as of the evolution of drug-induced resistance. In this connection, the complex **2** could represent a structural model worth to be further developed for the design and the development of new more promising anticancer drugs.

Experimental Section

Chemistry

All manipulations were performed under a dinitrogen atmosphere, if not otherwise stated. Solvents and liquid reagents were dried according to reported procedures.[40] ^{1}H-, ^{13}C-, ^{31}P- and ^{195}Pt NMR spectra were recorded with a Bruker ''Avance DRX400'' spectrometer, in $CDCl_3$ solution if not otherwise stated. Chemical shifts were measured in ppm (δ) from TMS by residual solvent peaks for ^{1}H and ^{13}C, from aqueous (D_2O) H_3PO_4 (85 %) for ^{31}P and from aqueous (D_2O) hexachloroplatinic acid for ^{195}Pt. A sealed capillary containing C_6D_6 was introduced in the NMR tube to lock the spectrometer to the deuterium signal when non-deuterated solvents were used. FTIR spectra in solid phase were recorded with a Perkin–Elmer ''Spectrum One'' spectrometer, equipped with an ATR accessory. Elemental analyses (C, H, N) were performed at Dipartimento di Scienze e Tecnologie Chimiche, Università di Udine and at Dipartimento di Chimica e Chimica Industriale, Università di Pisa. *Trans*-$[Pt(\mu\text{-}Cl)Cl(PPh_3)]_2$[21] was prepared according to a reported procedure. Oxime ligands from 2-hydroxybenzaldehyde (oxime I) and from 2-hydroxyacetophenone (oxime II) were prepared by a slight modification of a described procedure.[41] Silver acetate (98 %, Sigma Aldrich) was used without further purification.

General procedure for the synthesis of bidentate oxime complexes

A Schlenk tube equipped with a magnetic stirrer was charged with $[Pt(\mu\text{-}Cl)Cl(PPh_3)]_2$ (0.300-0.500 g), the suitable bidentate oxime (oxime/Pt = 1.03 molar ratio), silver acetate (AgOAc/oxime = 1.00 molar ratio) and 1,2-DCE. The mixture was shielded from light and stirred at 25 °C. A yellow solution was obtained and a colorless solid formed almost immediately. The suspension was stirred until the maximum conversion was reached (^{31}P-NMR, 2 h), then was filtered on a short package of celite. The liquid phase was concentrated under vacuum up to one third of the original volume and then treated with heptane. The yellow solid precipitated was filtered, washed with heptane and dried under vacuum.

(*SP*4-3)-[PtCl(PPh$_3$){(κ^2-*N,O*)-[1-(2-hydroxyphenyl)ethanone oxime]}] (**1**): From oxime II, 47% yield. $C_{26}H_{23}ClNO_2PPt{\cdot}C_2H_4Cl_2{\cdot}H_2O$ Anal. Calc.: C 44.3, H 3.9, N 1.8 %. Exp.: C 44.1, H 4.2, N 2.0 %. IR (ν, cm-1): 3231; 3055; 2963; 2906; 1596; 1541; 1504; 1482; 1475; 1460; 1434; 1398; 1341; 1314; 1260; 1234; 1185; 1136; 1096; 1014; 957; 866; 797; 755; 749; 708; 690. ^{1}H-NMR: 10.84 (d, 1H, J=2.9 Hz, OH); 7.80-7.76 (m, 6H, H_{arom}); 7.54-7.47 (m, 10H, H); 7.02 (t, 1H, H_{arom}); 6.66 (t, 1H, H_{arom}); 6.22 (d, 1H, J=8.4 Hz, H_{arom}); 2.51 (s, 3H, CH_3). ^{13}C-NMR: 161.4; 134.8 (d, J=10.6 Hz); 131.5; 131.1; 129.1; 128.2 (d, J=11.3 Hz);127.6 (d, J=63.6 Hz); 121.1; 119.7; 116.8; 43.4. ^{31}P-NMR: 6.65 ($^{1}J_{P\text{-}Pt}$ = 3959Hz). ^{195}Pt NMR: -2984 ($^{1}J_{P\text{-}Pt}$ = 3959 Hz).

(*SP*4-3)-[PtCl(PPh$_3$){(κ^2-*N,O*)-[(1E)-2-hydroxybenzaldehyde oxime]}] (**2**): From oxime I, 62 % yield. $C_{25}H_{21}ClNO_2PPt{\cdot}H_2O$ Anal. Calc.: C 46.4,

H 3.6, N 2.2 %. Exp.: C 46.2, H 3.6, N 2.2 %. IR (ν, cm-1): 3243; 3061; 1638; 1600; 1546; 1489; 1483; 1471; 1433; 1347; 1326; 1289; 1195; 1153; 1130; 1101; 1011; 999; 949; 914; 846; 816; 746; 732; 709. ^{1}H NMR: 10.63 (d, 1H, J=2.8 Hz, OH); 8.30 (d, 1H, J=9.7 Hz, CHN); 7.81-7.76 (m, 6H, H_{arom}); 7.55-7.46 (m, 9H, H_{arom}); 7.19-7.13 (m, 2H, H_{arom}); 6.62 (t, 1H, H_{arom}); 6.30 (d, 1H, J=8.5 Hz, H_{arom}). ^{13}C NMR: 144.5; 134.9 (d, J=10.6 Hz); 132.9 (d, J=57 Hz); 131.2; 128.2 (d, J=11.3 Hz); 127.7; 122.7; 120.1; 116.4; 115.6. ^{31}P NMR: 6.92 ($^{1}J_{P\text{-}Pt}$=3888 Hz). ^{195}Pt NMR: -2929 ($^{1}J_{P\text{-}Pt}$=3888 Hz).

X-Ray determinations

Crystals of **1** were selected at room temperature (296 K), glued to glass fibers and analyzed with a Bruker Smart Breeze CCD diffractometer. Table 3 summarizes the lattice parameters and the space group. Intensity data were collected in the range of 2θ angles reported in Table 3. After correction for Lorentz and polarization effects and for absorption, the structure solution was obtained using the direct methods contained in SHELXS program.[42] The hydrogen of oxime hydroxyl residue was found in the difference Fourier map, while the other hydrogen atoms were introduced in calculated positions. The final reliability factors of the refinement procedure, done using SHELXL program,[43] are listed in Table 3. Other control calculations were performed with the programs contained in the WINGX suite.[44]

CCDC **1988534** for **1** contains the supplementary crystallographic data for this paper. These data can be obtained free of charge from The Cambridge Crystallographic Data Centre.

Main Text Paragraph.

Table 3. Crystal data and structure refinement for complex **1.**

Compound	**1**	
Empirical formula	$C_{26}H_{23}ClNO_2PPt$	
Formula weight	642.96	
Temperature	296(2) K	
Wavelength	0.71073 Å	
Crystal system	Monoclinic	
Space group	$P\,2_1/c$	
Unit cell dimensions	a = 13.4469(5) Å	α= 90°.
	b = 10.4149(3) Å	β= 108.797(2)°.
	c = 19.5997(7) Å	γ = 90°.
Volume	2598.50(16) Å^3	
Z	4	
Density (calculated)	1.644 Mg/m^3	
Absorption coefficient	5.586 mm^{-1}	
F(000)	1248	
Crystal size	0.370 x 0.200 x 0.120 mm^3	
Theta range for data collection	2.954 to 29.591°.	
Index ranges	-18<=h<=13, -14<=k<=13, -23<=l<=27	
Reflections collected	25513	
Independent reflections	7256 [R(int) = 0.0298]	
Completeness to theta = 25.242°	99.8 %	
Refinement method	Full-matrix least-squares on F2	
Data / restraints / parameters	7256 / 0 / 289	
Goodness-of-fit on F^2	0.939	
Final R indices [I>2sigma(I)]	R1 = 0.0309, wR2 = 0.0823	
R indices (all data)	R1 = 0.0556, wR2 = 0.0950	
Extinction coefficient	n/a	
Largest diff. peak and hole	1.609 and -0.907 e.Å^{-3}	

Biological assays

Cell cultures: HeLa (human cervix adenocarcinoma) were grown in Ham's F12 Nutrient Mixture (Sigma Chemical Co. N6760); MSTO-211H (human biphasic mesothelioma) and MeT-5A (human mesothelial cells) were grown in RPMI 1640 (Sigma Chemical Co. R6504) supplemented with 2.38 g/L Hepes, 0.11 g/L pyruvate sodium and 2.5 g/L glucose; HT-29 (colorectal cancer), A2780 (human ovarian carcinoma) and A2780cis (human ovarian carcinoma cisplatin-resistant) were grown in RPMI 1640 (Sigma Chemical Co. R6504); A-549 (non-small cell lung cancer) were grown in Ham's F12 Nutrient Mixture (Sigma Chemical Co. N3520). 1.5 g/L $NaHCO_3$, 10% heat-inactivated fetal bovine serum (Biowest), 100 U/mL penicillin, 100 µg/mL streptomycin, and 0.25 µg/mL amphotericin B (Sigma Chemical Co. A5955) were added to the media. Cells were cultured at 37 °C in a moist atmosphere of 5% carbon dioxide in air.

Inhibition growth assay: Cells (2.5–3 x 10^4) were seeded into each well of a 24-well cell culture plate. After incubation for 24 h, different concentrations (from 0.1 to 20 µM) of the test complexes were added to the complete medium and incubated for a further 72 h. Stock solutions of new complexes were made in dimethylsulfoxide at 20 mM concentration and then diluted with complete medium in such a way that the final amount of solvent in each well did not exceed 0.5%. Cisplatin was dissolved in 0.9% NaCl. A Trypan blue assay was performed to determine cell viability. In detail, after 72 h of incubation with test complex, the medium was discarded and the cells were washed with Phosphate Buffer Saline. The cells were then harvested and 0.1% Trypan blue solution and cell suspension were mixed. A drop of the mixture was applied on a Burker counting chamber (Blau Brand, Germany) and viable (unstained) cells were counted within 3-5 minutes. Cytotoxicity data were expressed as IC_{50} values, i.e., the concentration of the test agent inducing 50% reduction in cell number compared with control cultures.

Nucleic acids: DNA from salmon testes was purchased from Sigma Chemical Co (D1626) and its concentration was determined using extinction coefficient 6600 $M^{-1}cm^{-1}$ at 260 nm. pBR322 DNA was purchased from Fermentas Life Sciences, its concentration was determined according to the manifacturer's indication.

Platinum and phosphorus binding to DNA: The quantitative platinum and phosphorus analyses were performed according to a previous

established method.[32] Briefly, an aqueous solution of salmon testes DNA (9 x 10^{-4} M) was incubated at 37 °C with test compound (stock solution 20 mM in DMSO) or cisplatin (stock solution 4 mM in 0.9% NaCl) to reach a [DNA]/ [drug] = 10. At fixed incubation time, aliquots of exact volume were collected and DNA was precipitated with Na-acetate (up to 0.3 M concentration) and cold ethanol (2 vol). The precipitated DNA was washed with 70% ethanol, dried and then dissolved in 250 μL of milliQ® water. The samples were then mineralized by treating with 195 μL HNO_3 (65%) at 90 °C for 20 min. Finally, the samples were diluted in 3 volumes of HCl (37%), and milliQ® water was added up to 5 mL. The analyses of P and Pt were performed by inductively coupled plasma atomic emission spectrometry (ICP-AES) at emission lines λ (P) = 178.290 nm and λ (Pt) = 214.423 nm. A Spectroflame Modula sequential and simultaneous ICP-spectrometer (ICP SPECTRO Arcos with EndOnPlasma torch) equipped with a capillary cross-flow Meinhard nebulizer was used (Spectro Analytical). Analytical determinations were performed using a plasma power of 1.2 kW, a radiofrequency generator of 27.12 MHz and an argon gas flow with nebulizer, auxiliary, and coolant set at 1, 0.5 and 14 L/min, respectively. Calibration was carried out by preparing 15 multielement standard solutions containing platinum and phosphorous in the concentration range 0–800 mg L^{-1} (ppm). Standard solutions were prepared by diluting phosphorous and platinum stock solutions of 1,000 mg L^{-1} (Spectrascan standards from Teknolab, Norway) with 1% HCl–water solution.[32] The concentrations reported for platinum and phosphorous as a function of incubation time are the mean values of three different experiments.

Unwinding assay: Supercoiled pBR322 plasmid DNA (80 ng) was incubated in aqueous solution with test compounds at indicated concentrations for 24 h at 37 °C in 20 μL final volume. 3 μL of loading buffer (0.125% bromophenol blue, 0.125% xylene cyanol and 50% glycerol) was added to each sample and DNA was separated by electrophoresis on a 1% agarose gel at room temperature. The gels were stained with ethidium bromide (1 μg/mL) in TA buffer (0.04 M Tris and 0.02 M Acetic Acid), transilluminated by UV light, and the fluorescence emission was visualized by a CCD camera coupled to a Bio-Rad Gel Doc XR apparatus.

Cell uptake: A2780cis cells (2 x 10^6) were seeded into each cell culture plate in complete growth medium. After incubation for 24 h the test agents were added to the complete medium at 100 μM concentration. At fixed incubation time (0-180 min), the cells were harvested, washed twice with 0.9% NaCl and the pellet mineralized by treating with 195 μL of HNO_3 (65%) at 90 °C for 1 h. Finally, the samples were diluted in 3 volumes of HCl (37%), and milliQ® water was added up to 5 mL. The content of P and Pt were performed by inductively coupled plasma atomic emission spectrometry (ICP-AES) at emission lines λ (P) = 178.290 nm and λ (Pt) = 214.423 nm, as described in Platinum and phosphorus binding to DNA section.

Mitochondrial transmembrane potential measurement: The mitochondrial transmembrane potential was assayed by BD™ MitoScreen Kit (BD Pharmigen), according to Cossarizza et al.[45] Briefly, A2780cis cells (3 × 10^5) were seeded and incubated in standard medium for 24 h. The test agents were added at the indicated concentrations and drug-treated cells were incubated for a further 28 h. The cells were then centrifuged, resuspended in JC-1 Working Solution and incubated for 30 min at 37 °C in the dark. Following incubation, cells were washed twice in Assay buffer, resuspended and immediately analyzed by a FACSCanto II flow cytometer (Becton-Dickinson, Mountain View, CA). Ten thousand events per sample were analysed.

Preparation of cytosol and mitochondria enriched fractions and analysis of platinum and phosphorus content: A2780cis cells (5 x 10^6) were seeded into 75 cm^2 cell flasks and cultured for 24 h. Then, cells were treated with the complexes (100 μM) in a complete medium, for 3 h. Subsequently, cells were harvested and sub-fractionated following the protocol of Clayton and Shadel[46] as modified by Scalcon et al.[47] Briefly, cells (3x10^7 per condition) were collected, washed with PBS, subjected to hypo-osmotic treatment with 1 mL of 10 mM NaCl, 1.5 mM $MgCl_2$, 10 mM Tris-HCl buffer (pH 7.5) for 5 min and gently homogenized using a Dounce tissue grinder. Afterwards, 0.7 mL of 525 mM mannitol, 175 mM sucrose, 2.5 mM EDTA, 12.5 mM Tris-HCl buffer (pH 7.5) were rapidly added. The homogenate was diluted to a final volume of 2.5 mL with 210 mM mannitol, 70 mM sucrose, 1 mM EDTA, 5 mM Tris-HCl buffer (pH 7.5) and subjected to differential centrifugation. The first step was carried out at 1300g for 5 min at 4 °C to obtain the crude nuclear fraction (containing also non-disrupted cells). The mitochondrial fraction was pulled down from the supernatant (cytosolic fraction) at 15800g for 15 min at 4°C and washed twice. Mitochondrial pellets were mineralized by treating with 195 μL of HNO_3 (65%) at 90 °C for 1 h. Then, the samples were diluted in 3 volumes of HCl (37%), and milliQ® water was added up to 5 mL. Cytosol fractions (2.5 mL) were mineralized by treating with 1.95 mL of HNO_3 (65%) at 90 °C for 1 h. Finally, HCl (37%) was added up to 5 mL. The P and Pt content was determined. The analyses of P and Pt were performed by inductively coupled plasma atomic emission spectrometry (ICP-AES) at emission lines λ (P) = 178.290 nm and λ (Pt) = 214.423 nm, as described in Platinum and phosphorus binding to DNA section.

Reactive Oxygen Species formation: A2780cis cells (1 x 10^4 per well) were seeded into a p96 cell culture plate in complete growth medium. After incubation for 24 h, the medium was removed and the cells washed with phosphate buffered saline (PBS). Cells were incubated with 10 μM of the fluorogenic probe CM-H_2DCFDA (Molecular Probes, Thermo Fisher Scientific) in PBS-glucose 10 mM at 37 °C in the dark for 20 min, washed with PBS, and incubated with test agent at the indicated concentrations in PBS/glucose 10 mM. Fluorescence increase was detected by a plate reader (Tecan Infinite® M200 PRO, Männedorf, CH) at 485 nm (λ excitation) and 527 nm (λ emission).

Acknowledgements

L.D.V. is grateful for the financial support provided by Dipartimento di Scienze del Farmaco, Università di Padova Progetti di Ricerca di Dipartimento – PRID 2017 DALL_SID17_02– “An in depth investigation on novel Pt-based agents to shed light on cancer resistance mechanisms” and thanks the Consorzio Interuniversitario di Ricerca in Chimica dei Metalli nei Sistemi Biologici (CIRCMSB). Pisa University (Fondi di Ateneo 2018 and Progetti di Ricerca di Ateneo 2017—PRA_2017_25) is gratefully acknowledged.

Keywords: platinum • bioinorganic chemistry • cytotoxicity • drug resistance • mitochondria

[1] A.W. Prestayko, J.C. D'Aoust, B.F. Issell, S.T. Crooke, *Cancer Treat. Rev.* **1979**, *6*, 17–39.
[2] D. Lebwohl, R. Canetta, *Eur. J. Cancer* **1998**, *34*, 1522–1534.
[3] M. Galanski, *Recent Patents Anti-Canc. Drug Discov.* **2006**, *1*, 285–295.
[4] M.D. Hall, M. Okabe, D.W. Shen, X.J. Liang, M.M. Gottesman, *Annu. Rev. Pharmacol. Toxicol.* **2008**, *48*, 495-535.
[5] L. Kelland, *Drugs* **2000**, *59*, 1–8.
[6] S. Dasari, P.B. Tchounwou, *Eur. J. Pharmacol.* **2014**, *740*, 364-378.
[7] L. Kelland, *Nat. Rev. Cancer* **2007**, *7*, 573-584.
[8] L. Galluzzi, L. Senovilla, I. Vitale, J. Michels, I. Martins, O. Kepp, M. Castedo, G. Kroemer, *Oncogene* **2012**, *31*, 1869-1883.
[9] S. Fulda, L. Galluzzi, G. Kroeme, *Nat. Rev. Drug Discov.* **2010**, *9*, 447-464.
[10] P. Costantini, E. Jacotot, D. Decaudin, G. Kroemer, *J. Natl. Cancer Inst.* **2000**, *92*, 1042-53
[11] D. Pathania, M. Millard, N. Neamati, *Adv. Drug Deliv. Rev.* **2009**, *61*, 1250-1275.

[12] M.F.C. Guedes da Silva, Y. A. Izotova, A.J.L. Pombeiro, V.Y. Kukushkin, *Inorg. Chim. Acta* **1998**, 277, 83-88.
[13] Kukushkin, D. Tudela, Y.A. Izotova, V.K. Belsky, A.I. Stash, *Polyhedron*, **1998**, 17, 2455-2461.
[14] E. Borre, G. Dahm, G. Guichard, S. Bellemin-Laponnaz *New J. Chem.* **2016**, *40*, 3164-3171.
[15] D.A. Erdogan, S. Ozalp-Yaman *J. Mol. Struct.* **2014**, *1064*, 50-57.
[16] G. Grabmann, S.M. Meier, Y.Y. Scaffidi-Domianello, M. Galanski, B.K. Keppler, C.G. Hartinger *J. Chromatogr A* **2012**, *1267*, 156-161.
[17] C. Bartel, A.K. Bytzek, Y.Y. Scaffidi-Domianello, G. Grabmann, M.A. Jakupec, C.G. Hartinger, M. Galanski, B.K. Keppler, *J. Biol. Inorg. Chem.* **2012**, *17*, 465-474.
[18] Y.Y. Scaffidi-Domianello, A.A. Legin, M.A. Jakupec, V.B. Arion, V.Y. Kukushkin, M. Galanski, B.K. Keppler, Inorg. Chem. **2011**, *50*, 10673-10681.
[19] D. Belli Dell'Amico, M. Colalillo, L. Dalla Via, M. Dell'Acqua, A. N. García-Argáez, M. Hyeraci, L. Labella, F. Marchetti, S. Samaritani, *Eur. J. Inorg. Chem.* **2018**, 1589–1594.
[20] L. Dalla Via, A. N. García-Argáez, A. Adami, S. Grancara, P. Martinis, A. Toninello, D. Belli Dell'Amico, L. Labella, S. Samaritani, *Bioorg. Med. Chem*. **2013**, *21*, 6965-6972.
[21] D. Belli Dell'Amico, L. Labella, F. Marchetti, S. Samaritani, *Dalton Trans.* **2012**, *41*, 1389-1396.
[22] D. Belli Dell' Amico, M. Colalillo, L. Labella, F. Marchetti, S. Samaritani, *Inorg. Chim. Acta* **2018**, *47030*, 181-186
[23] S. F. Kaplan, V. Y. Kukushkin, S. Shova, K. Suwinska, G. Wagner, A. J. L. Pombeiro, *Eur. J. Inorg. Chem.* **2001**, 1031-1038.
[24] M.V. Keck, S.J. Lippard, *J. Am. Chem. Soc.* **1992**, *114*, 3386-3390.
[25] D.W. Shen, L.M. Pouliot, M.D. Hall, M.M. Gottesman, *Pharmacol. Rev.* **2012**, *64*, 706-721.
[26] J. Zisowsky, S. Koegel, S. Leyers, K. Devarakonda, M.U. Kassack, M. Osmak, U. Jaehde, *Biochem. Pharmacol*. **2007**, *73*, 298-307.
[27] S. Fulda, K.M. Debatin, *Oncogene* **2006**, *25*, 4798-4811.
[28] Z.H. Siddik in *Cancer Drug Discovery and Development: Cancer Drug Resistance* (Ed.: B. Teicher) Humana Press Inc., Totowa, NJ, **2006**, pp. 283-307.
[29] R.W. Horobin, S. Trapp, V. Weissig, *J. Control. Release* **2007**, *121*, 125-136.
[30] J.D. Robertson, V. Gogvadze, B. Zhivotovsky, S. Orrenius, *J. Biol. Chem.* **2000**, *275*, 32438-32443.
[31] J.F. Kidd, M.F. Pilkington, M.J. Schell, K.E. Fogarty, J.N. Skepper, C.W. Taylor, P. Thorn, J. *Biol. Chem.* **2002**, *277*, 6504-10.
[32] L. Dalla Via, S. Santi, V. Di Noto, A. Venzo, E. Agostinelli, A. Calcabrini, M. Condello, A. Toninello, *J. Biol. Inorg. Chem.*, **2011**, *16*, 695-713.
[33] M.P. Murphy, *Trends Biotechnol.* **1997**, *15*, 326-330.
[34] R.A. Smith, C.M. Porteous, A.M. Gane, M.P. Murphy, *Proc. Natl. Acad. Sci. U. S. A.* **2003**, *100*, 5407-5412.
[35] M.C. Frantz, P. Wipf, *Environ. Mol. Mutagen*. **2010**, *51*, 462-475.
[36] V. Scalcon, A. Bindoli, M.P. Rigobello *Free Radic. Biol. Med.* **2018**, *127*, 62-79.
[37] L. A. Sena, S.N.S. Chandel, *Mol. Cell* **2012**, *48*, 158-167.
[38] J. Zhang, X. Wang, V. Vikash, Q. Ye, D. Wu, Y. Liu, W. Dong, *Oxidative Med. Cell. Longev*. **2016**, *2016*, 4350965.
[39] M. Redza-Dutordoir, D.A. Averill-Bates, *Biochim. Biophys. Acta* **2016**, *1863*, 2977-2992.
[40] W. L. F. Armarego, D. D. Perrin in *Purification of Laboratory Chemicals*, Butterworth-Heinemann, **1996**.
[41] C. B. Aakeröy, A. S. Sinha, *RSC Adv*. **2013**, *3*, 8168-8171.
[42] G. M. Sheldrick, SHELXS. Version 2014/7 2013, Georg-August-Universität Göttingen, Göttingen, Germany.
[43] G.M. Sheldrick, SHELXL (Release 97–2) 1998, University of Göttingen, Göttingen, Germany.
[44] L.J. Farrugia, *J. Appl. Crystallogr.* **1999**, *32*, 837-838.
[45] A. Cossarizza, M. Baccaranicontri, G. Kalashnikova, C. Franceschi, *Biochem. Biophys. Res. Commun.*, **1993**, *197*, 40-45.
[46] D.A. Clayton, G.S. Shadel in *Cold Spring Harbor Protocols,* **2014**, 74542.
[47] V. Scalcon, M. Salmain, A. Folda, S. Top, P. Pigeon, H.Z.S. Lee, G. Jaouen, A. Bindoli, A. Vessieres, and M.P. Rigobello, *Metallomics*, **2017**, *9*, 949-959.

10.1002/cmdc.202000165

WILEY-VCH

Table of Contents

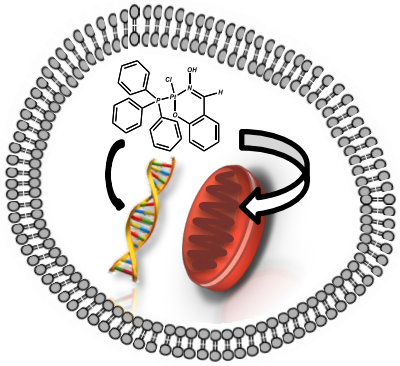

Fighting drug resistance. The Pt(II) complex efficiently enters into resistant cells causing significant antiproliferative effect, despite scarce interaction with DNA. Mitochondria appear a possible target. Mitochondrial membrane depolarization and oxidative stress seem responsible for cytotoxicity. This biological profile could represent a model for the development of promising anticancer drugs.